Available online at www.sciencedirect.com

ScienceDirect

Nuclear and Particle Physics Proceedings 273–275 (2016) 1565–1570

www.elsevier.com/locate/nppp

Soft probes of the QGP: Pb-Pb and p-Pb CMS results

J. Milošević on behalf of the CMS Collaboration

Vinca Institute of Nuclear Sciences
University of Belgrade
M. Petrovica Alasa 12-14
P. O. Box 522
11001 Belgrade, Serbia

Abstract

The CMS collaboration measured second-order single-particle anisotropy, v_2, using 2-, 4-, 6- and 8-particle correlations as well as the Lee-Yang Zero method in pPb and PbPb collisions. This result shows that the correlations found in the small and highly asymmetric pPb collision system are long-range and have a many-particle origin. Deeper insight into the nature of these correlations is achieved by studying the factorization breaking effect which appears trough a p_T-dependent event plane angle, caused by the initial-state fluctuations. The effect is largest for the most-central PbPb collisions (up to 20%), while it is on the level of few percent for peripheral PbPb and high-multiplicity pPb events. Hydrodynamics models which include a p_T-dependent event plane angle semi-quantitatively describe the data and suggest that the effect is mainly determined by the initial-state conditions.

Keywords: flow, CMS, two-particle correlations, multi-particle-correlations, factorization breaking

1. Introduction

The Quark-Gluon Plasma (QGP), formed in the relativistic heavy-ion collisions, undergoes a collective expansion which is called flow. In such collisions, colliding nuclei intersect in such as way as to form a spatially anisotropic overlap region, which due to the interactions between the constituents of the formed system, converts into a momentum anisotropy. As a consequence, particles are preferentially emitted in the plane with the biggest pressure gradient. This plane is called the event plane (EP) and it is characterized via its azimuthal angle Ψ_n. The final azimuthal angle particle distribution can be Fourier decomposed as

$$\frac{dN}{d\phi} \propto 1 + 2\sum_{n=1}^{\infty} v_n \cos[n(\phi - \Psi_n)] \tag{1}$$

A most significant part of the composite signal comes from the second Fourier component, v_2, called 'elliptic flow'. Due to the initial-state fluctuations, the overlap region is not perfectly lenticular which as a consequence have appearance of higher orders Fourier coefficients. The third Fourier component, the triangular flow, v_3, appears to be a significant source of the overall signal too, especially in the central collisions.

If particles are correlated with the event plane, then they are also mutually correlated. This enables the use of the two- and multi-particle correlations as a promising tool to study collective phenomena in relativistic protons and nuclei collisions. Two dimensional (2D) particle correlations in $\Delta\phi$ and $\Delta\eta$, which are differences in azimuthal angle ϕ and in pseudorapidity η between particles in a pair, have a rich structure. Especially, it showed existence of the ridge,

http://dx.doi.org/10.1016/j.nuclphysbps.2015.09.253
2405-6014/

long-range structure in $|\Delta\eta|$ in vicinity of $\Delta\phi$=0, in both PbPb (1) and pPb (2) collisions. A similar correlation has been found even in the smallest pp system (3) with very high multiplicity. In order to avoid short-range correlations arising from jet fragmentation for example, a cut on $|\Delta\eta|$ could be applied[1]. Then, performing a projection of the constructed 2D particle correlations onto the $\Delta\phi$ axis, we obtain azimuthal correlations of particle pairs which could also be characterized by a Fourier decomposition

$$\frac{dN}{d\Delta\phi} \propto 1 + 2\sum_{n=1}^{\infty} V_{n\Delta}\cos(n\Delta\phi) \tag{2}$$

The results in this contribution are, in fact, obtained by the direct calculations of Fourier coefficients $V_{n\Delta}$ as

$$V_{n\Delta} = \langle\langle\cos(n\Delta\phi)\rangle\rangle_S - \langle\langle\cos(n\Delta\phi)\rangle\rangle_B \tag{3}$$

where $\langle\langle ...\rangle\rangle$ means averaging over many pairs and over many events of interest. The indices S and B stand for *signal* and *background*. The background distribution is calculated in the same way as the signal one with the only difference that particles forming a pair are taken from different events with similar multiplicities and within 2 cm wide range of vertex position in the z direction. The subtraction of the background takes into account the effects of detector non-uniformity. The direct calculation of $V_{n\Delta}$ has an advantage that it is not affected by the finite bin widths of the $\Delta\phi - \Delta\eta$ histogram, which is especially relevant for higher-order Fourier harmonics.

Beside the two-particle correlations, there are methods which use many-particle correlations in order to extract the magnitudes of the Fourier coefficients. In this contribution, the corresponding cumulants, $c_n\{2k\}, k = 2, 3, 4$ are calculated according to the prescription described in detail in (4, 5).

The hydrodynamics is usually used to explain seen phenomena in large nucleus-nucleus collision system, while different theoretical models are trying to explain it for the small systems formed in pp or pPb collisions. Usual assumption that EP angle Ψ_n does not depend on p_T leads to factorization

$$V_{n\Delta}(p_{T1}, p_{T2}) = \sqrt{V_{n\Delta}(p_{T1}, p_{T1})} \times \sqrt{V_{n\Delta}(p_{T2}, p_{T2})} = v_n(p_{T1}) \times v_n(p_{T1}) \tag{4}$$

of two-particle Fourier coefficients, $V_{n\Delta}$, from Eq.(2) in a product of single-particle Fourier coefficients from Eq.(1). Recently, it was shown in (6) and (7) that not only v_n but also the EP angle Ψ_n could depends on p_T. Due to the initial-state fluctuations, even if the only source of the correlations is hydrodynamic motion, the Ψ_n is not any more a plane common for the whole event and its value becomes p_T dependent. In that case, Eq.(4) becomes inequality

$$V_{n\Delta}(p_{T1}, p_{T2}) = \langle v_n(p_{T1}) v_n(p_{T2}) \cos[n(\Psi_n(p_{T1}) - \Psi_n(p_{T2}))]\rangle \neq \sqrt{V_{n\Delta}(p_{T1}, p_{T1})} \times \sqrt{V_{n\Delta}(p_{T2}, p_{T2})} \tag{5}$$

and factorization is broken. A newly proposed variable

$$r_n = \frac{V_{n\Delta}(p_{T1}, p_{T2})}{\sqrt{V_{n\Delta}(p_{T1}, p_{T1})}\sqrt{V_{n\Delta}(p_{T2}, p_{T2})}} = \frac{\langle v_n(p_{T1}) v_n(p_{T2}) \cos[n(\Psi_n(p_{T1}) - \Psi_n(p_{T2}))]\rangle}{\sqrt{v_n^2(p_{T1}) v_n^2(p_{T2})}} \tag{6}$$

is used to measure directly the magnitude of the factorization breaking effect. As single-particle anisotropy coefficients are mainly canceled, the r_n is approximately equal to $\cos[n(\Psi_n(p_{T1}) - \Psi_n(p_{T2}))]$. In the case where the effect is entirely driven by the collective flow, the r_n achieved value smaller (equal) than one when factorization breaks (holds). The r_n value greater than one means that there are unremoved non-flow effects.

2. The CMS experiment and data used

The CMS detector consists out of several subdetectors (8) and it is placed within a super-conducting solenoid which produces 3.8 T magnetic field enabling precise measurements of particle momenta. The analysis, presented in this paper, is performed using data collected by CMS experiment at the LHC energies of $\sqrt{s_{NN}}$ = 2.76 TeV and 5.02 TeV in PbPb and pPb with integrated luminosities of 160 μb^{-1} and 35 nb^{-1}, respectively.

[1] In this analysis, thanks to a large CMS coverage in η, a wide $|\Delta\eta|$ >2.0 cut has been applied.

The data used in this analysis comes mainly from the silicon tracker. The silicon tracker measures charged particles with pseudorapidities from the range $|\eta| < 2.5$ and transverse momenta above 0.3 GeV/c. The detailed information on cuts used for the online triggers, offline event selections, track reconstruction and selections are listed in (9) and (10). The multiplicity classes are formed based on track multiplicity, $N_{trk}^{offline}$, where only primary tracks with $|\eta|$ <2.4 and p_T >0.4 GeV/c are counted. More details on multiplicity classification can be found in (5).

3. Results

CMS measured the second-order single-particle anisotropy, v_2, using the two- and higher order (4-th, 6-th and 8-th) particle correlations as well as the Lee-Yang Zero method both in PbPb and in pPb collisions over a wide multiplicity interval (9). These results, obtained by averaging over $0.3 < p_T < 3.0$ GeV/c and within $|\eta|$ <2.4, are shown in Fig. 1. It is found that values of $v_2\{4\}$, $v_2\{6\}$, $v_2\{8\}$ and $v_2\{LYZ\}$ are in a very good mutual agreement. Also, they are consistently below the corresponding $v_2\{2\}$ values. This result shows that correlations found in the small and highly asymmetric pPb collision system are long-range and have a many-particle origin. All applied methods show that v_2 increases with increase of multiplicity in PbPb collisions. In pPb collisions, the $v_2\{2\}$ has a modest increase, while v_2 from higher order particle correlations stays nearly constant with multiplicity. Such different behavior could be explained by the presence of lenticular shape of the overlapping region in PbPb collisions, while in the case of pPb collisions the shape of the overlapping region is determined by the initial-state fluctuations.

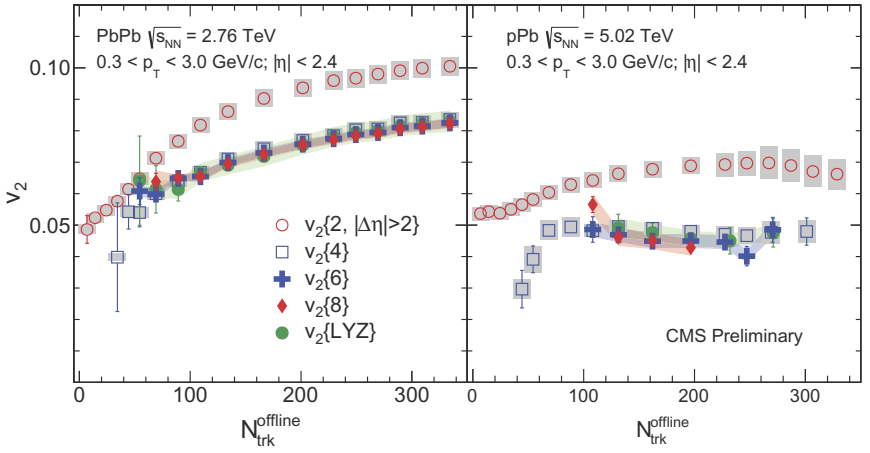

Figure 1: The v2 measured from two-, four-, six- and eight-particle correlations as well as using the LYZ method *vs* $N_{trk}^{offline}$ multiplicity for $0.3 < p_T < 3.0$ GeV/c from PbPb (left) and pPb (right) data collected by CMS detector.

The very first experimental measurement of the factorization breaking has been performed for PbPb collisions at $\sqrt{s_{NN}}$=2.76 TeV in (11). In this contribution, the analysis is expanded to a much wider centrality range. Also, the effect is studied for high multiplicity pPb collisions at $\sqrt{s_{NN}}$=5.02 TeV. A systematic comparison between the experimental data and two hydrodynamic models (7, 12) is also included. To quantify the effect of the factorization breaking, the r_n observable is plotted *vs* the transverse momentum difference, $p_T^{trig} - p_T^{assoc}$, between the particles forming pairs of interest. By construction, $r_n = 1$ when trigger and associated particle belongs to the same p_T interval. Also, the calculations are performed only for $p_T^{trig} \geq p_T^{assoc}$.

The p_T-dependent results on factorization ratio r_2 and r_3 can be found in Fig. 4 and Fig. 5 respectively in (10)[2]. The shown error bars correspond to statistical uncertainties only, as the systematic uncertainties are negligible with respect to the statistical ones. In the case of r_2, the size of the effect increases with an increase of the difference between p_T^{trig} and p_T^{assoc}, with p_T^{trig} and going to more central collisions. The maximal effect of ≈20% is achieved in ultra-central 0-0.2% collisions. For centralities below 5%, the size of the effect is at the level of few %. In the case

[2]Due to the limited space these figures are not shown in this contribution

of third-order harmonic the factorization holds better then in the case of the second-order harmonic. The r_3 shows a very weak centrality dependence with the biggest value of about 5% at large values of $p_T^{trig} - p_T^{assoc}$.

In order to get better insights on the origin of long-range correlations observed in high-multiplicity pPb collisions, the r_2 and the r_3 measurements are also performed for high-multiplicity pPb collisions. The results for the r_2 in function of $p_T^{trig} - p_T^{assoc}$ are shown in Fig. 2. Four rows correspond to four analyzed multiplicity intervals, while four columns correspond to four different trigger's p_T. The r_2 shows factorization breaking of the similar size in all four multiplicity intervals. As in the case of PbPb collisions, the size of the effect increases with an increase of $p_T^{trig} - p_T^{assoc}$ and with p_T^{trig}. The maximal magnitude of the effect reaches only a few percent and it is much smaller than the one seen in ultra-central PbPb collisions, but it is comparable with the r_2 values found in those PbPb collisions which have multiplicities similar to high-multiplicity pPb events.

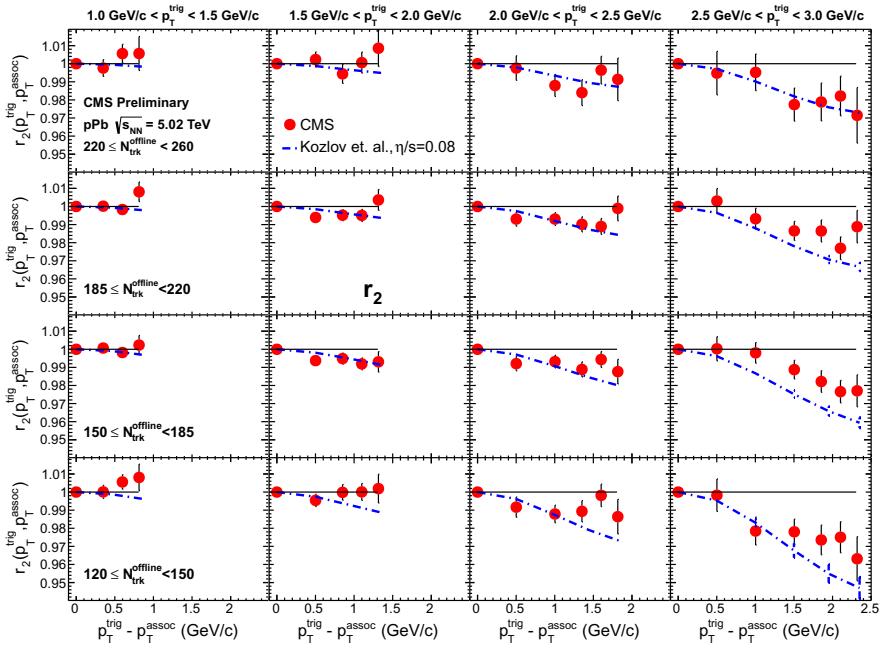

Figure 2: The p_T-dependent factorization ratio, r_2, as a function of $p_T^{trig} - p_T^{assoc}$ in bins of p_T^{trig} for four $N_{trk}^{offline}$ multiplicity ranges in 5.02 TeV pPb collisions. Predictions from hydrodynamic calculations for pPb collisions (12) are also shown with blue dot-dashed lines. The error bars correspond to statistical uncertainties, while systematic uncertainties are negligible for the r_n ratios, and thus are not presented in the figures.

The results of r_3, shown in Fig. 3, are presented in the same format as those for the r_2 ratio. Within currently available statistics, there is no significant factorization breaking in very high multiplicity pPb events ($185 < N_{trk}^{offline} < 260$). For lower multiplicity pPb events, particularly for $120 < N_{trk}^{offline} < 150$, the r_3 value exceeds one. This is a direct indication that there is a significant contributions of back-to-back jet correlations in the signal distributions used to extract the $V_{n\Delta}$ coefficients as the event multiplicity decreases, because the r_n ratios predicted by hydrodynamic models with a p_T-dependent event plane angle fluctuations would always be equal or less than one, according to Eq. 6.

Beside the experimental data points, in Fig. 2 and 3 are also shown predictions from Kozlov *et al.* hydrodynamic model (12). This model semi-quantitatively describes the experimental results. In Kozlov *et al.* model, a modified MC-Glauber initial-state model is used. The contributing entropy density in the transverse plane is distributed according to a 2D Gaussian distribution whose width can vary and which represents the transverse granularity of fluctuations. The experimentally found r_n ratios are found to be most sensitive just to that width. The r_2 data values are better described with a width parameter of 0.4 fm, while the width of 0.8 fm gives a r_n ratio practically equal to unity and thus underestimates the effect observed in the data. For both cases, the calculations are found to be nearly insensitive to different η/s values. This finding is consistent with the hydrodynamic calculations (7) used for more central PbPb collisions presented earlier. The results on factorization breaking in pPb collisions can provide new insight into the hydrodynamic nature of long-range correlations and the role of initial-state fluctuations in such a small system.

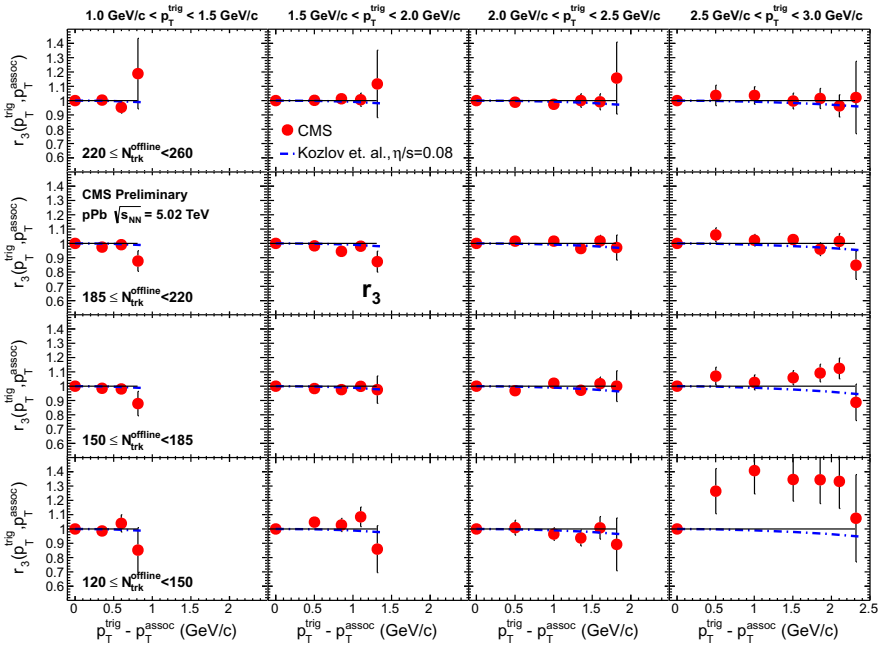

Figure 3: The p_T-dependent factorization ratio, r_3, as a function of $p_T^{trig} - p_T^{assoc}$ in bins of p_T^{trig} for four $N_{trk}^{offline}$ multiplicity ranges in 5.02 TeV pPb collisions. Predictions from hydrodynamic calculations for pPb collisions (12) are also shown with blue dot-dashed lines. The error bars correspond to statistical uncertainties, while systematic uncertainties are negligible for the r_n ratios, and thus are not presented in the figures.

In order to perform a quantitative study of factorization breaking effect *vs* multiplicity in PbPb and pPb collisions, the r_2 and r_3 ratios are evaluated where the effect reaches its maximum, i.e. for 2.5< p_T^{trig} <3.0 GeV/c and 0.3< p_T^{assoc} <0.5 GeV/c, or in other words for $p_T^{trig} - p_T^{assoc} \approx 2$ GeV/c. The obtained results are shown in Fig. 4. Additionally, at the top of the figure the centrality axis is shown which is applicable only for PbPb collisions. The r_2 factorization breaking effect in PbPb events increases dramatically as the collisions become more central than $0-5\%$. Going from central to peripheral PbPb collisions, the size of the r_2 effect quickly decreases to only few percent. The effect in r_3 remains at $2-3\%$ level and it is nearly independent of centrality. The hydrodynamic model predictions for PbPb collisions (7) with MC Glauber and MC-KLN initial conditions and η/s =0.12 are also shown in dashed lines as a function of centrality. Neither of the two used intial-state conditions can describe the data quantitatively, although the multiplicity dependence is qualitatively reproduced. In the case of pPb collisions, the r_2 ratios show little multiplicity dependence and they are consistent with predictions of Kozlov *et al.* hydrodynamic model (12). The r_3 ratios in pPb go significantly above 1 at lower multiplicities, due to the onset of non-flow correlations.

4. Summary

Using the CMS detector, the azimuthal dihadron correlations are studied as a function of transverse momentum in PbPb collisions at $\sqrt{s_{NN}}$ =2.76 TeV and pPb collisions at $\sqrt{s_{NN}}$ = 5.02 TeV. In this contribution the factorization of Fourier coefficients, $V_{n\Delta}$, into a product of single-particle azimuthal anisotropies, v_n, has been studied. A strong effect of r_2 factorization breaking, up to about 20%, is found in the case of ultra-central PbPb collisions. For peripheral PbPb collisions, as well as for high-multiplicity pPb collisions, the size of the effect is on the level of few percent. The data are semi-quantitatively described by hydrodynamic models, with p_T-dependent event plane angle fluctuations induced by initial-state fluctuations. These results can be used to constrain the transverse fluctuations in the initial nucleus-nucleus overlap region.

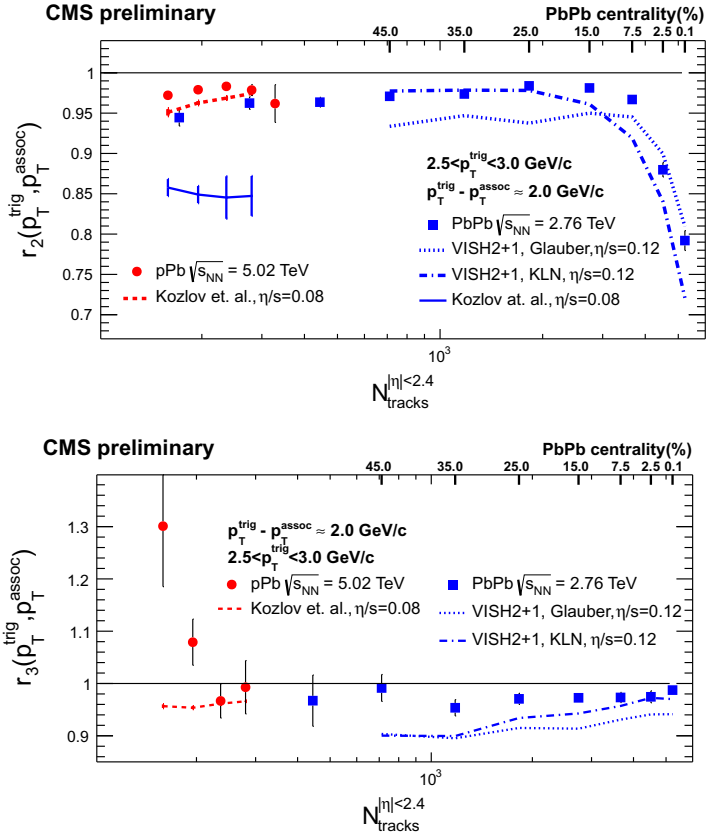

Figure 4: The p_T-dependent factorization ratio, r_2 (top) and r_3 (bottom) as a function of event multiplicity in pPb and PbPb collisions. The lines show the calculations for PbPb collisions from viscous hydrodynamics in Ref. (7) with MC-Glauber and MC-KLN initial condition models and $\eta/s = 0.12$, and also hydrodynamics predictions for pPb collisions with $\eta/s = 0.08$ (12).

References

[1] S. Chatrchyan, et al., Long-range and short-range dihadron angular correlations in central PbPb collisions at a nucleon-nucleon center of mass energy of 2.76 TeV, JHEP 1107 (2011) 076. arXiv:1105.2438, doi:10.1007/JHEP07(2011)076.

[2] S. Chatrchyan, et al., Observation of long-range near-side angular correlations in proton-lead collisions at the LHC, Phys.Lett. B718 (2013) 795–814. arXiv:1210.5482, doi:10.1016/j.physletb.2012.11.025.

[3] V. Khachatryan, et al., Observation of Long-Range Near-Side Angular Correlations in Proton-Proton Collisions at the LHC, JHEP 1009 (2010) 091. arXiv:1009.4122, doi:10.1007/JHEP09(2010)091.

[4] A. Bilandzic, R. Snellings, S. Voloshin, Flow analysis with cumulants: Direct calculations, Phys.Rev. C83 (2011) 044913. arXiv:1010.0233, doi:10.1103/PhysRevC.83.044913.

[5] S. Chatrchyan, et al., Multiplicity and transverse momentum dependence of two- and four-particle correlations in pPb and PbPb collisions, Phys. Lett. B 724 (2013) 213. arXiv:1305.0609, doi:10.1016/j.physletb.2013.06.028.

[6] F. G. Gardim, F. Grassi, M. Luzum, J.-Y. Ollitrault, Breaking of factorization of two-particle correlations in hydrodynamics, Phys.Rev. C87 (3) (2013) 031901. arXiv:1211.0989, doi:10.1103/PhysRevC.87.031901.

[7] U. Heinz, Z. Qiu, C. Shen, Fluctuating flow angles and anisotropic flow measurements, Phys. Rev. C 87 (2013) 034913. arXiv:1302.3535, doi:10.1103/PhysRevC.87.034913.

[8] S. Chatrchyan, et al., The CMS experiment at the CERN LHC, JINST 3 (2008) S08004. doi:10.1088/1748-0221/3/08/S08004.

[9] CMS Collaboration, Multiplicity dependence of multiparticle correlations in pPb and PbPb collisions, CMS Physics Analysis Summary HIN-14-006, CMS(2014).

[10] CMS Collaboration, Factorization breakdown of two-particle correlations in pPb and PbPb collisions at CMS, CMS Physics Analysis Summary HIN-14-012, CMS(2014).

[11] S. Chatrchyan, et al., Studies of azimuthal dihadron correlations in ultra-central PbPb collisions at $\sqrt{s_{NN}}$ = 2.76 TeV, JHEP 1402 (2014) 088. arXiv:1312.1845, doi:10.1007/JHEP02(2014)088.

[12] I. Kozlov, M. Luzum, G. Denicol, S. Jeon, C. Gale, Transverse momentum structure of pair correlations as a signature of collective behavior in small collision systems, arXiv:1405.3976.